Research Article | Vol. 8, No. 5 | 1 May 2017 | BIOMEDICAL OPTICS EXPRESS 2396
Biomedical Optics EXPRESS

Achromatic doublet intraocular lens for full aberration correction

ENRIQUE J. FERNANDEZ* AND PABLO ARTAL

Instituto de Investigación en Óptica y Nanofísica, Laboratorio de Óptica, Universidad de Murcia, Edificio 34, Campus de Espinardo, 30100 Murcia, Spain
**enriquej@um.es*

Abstract: A doublet intraocular lens optimized for both chromatic and monochromatic aberration correction in pseudophakic eyes is presented. Ray-tracing techniques were applied to design the lens in white light within a chromatic eye model. Combinations of two materials, already commonly used in intraocular lenses, as acrylic and silicone, were used. Iterative optimization algorithms were employed to correct for longitudinal chromatic aberration, spherical aberration and off-axis aberrations within 10 degrees of visual field. The performance of this lens was compared with a standard single-material aspheric intraocular lens. Near full aberration correction was achieved with the doublet intraocular lens. The modulation transfer function and Strehl ratio were superior for the doublet lens. Through-focus calculations were also conducted showing better optical quality for the doublet. Real higher-order aberrations from normal eyes were incorporated in the model to evaluate the effect on the doublet intraocular lens performance. Results showed that the doublet lens preserved its benefits under realistic conditions. This doublet intraocular lens should provide patients with a better quality of vision after it is further developed in terms of manufacturing and surgical limitations.

OCIS codes: (170.4460) Ophthalmic optics and devices; (330.7326) Visual optics, modeling; (330.7335) Visual optics, refractive surgery; (170.4470) Ophthalmology.

References and links

1. D. L. Cooke and T. L. Cooke, "Comparison of 9 intraocular lens power calculation formulas," J. Cataract Refract. Surg. **42**(8), 1157–1164 (2016).
2. K. J. Hoffer, "The Hoffer Q formula: A comparison of theoretic and regression formulas," J. Cataract Refract. Surg. **19**(6), 700–712 (1993).
3. J. A. Retzlaff, D. R. Sanders, and M. C. Kraff, "Development of the SRK/T intraocular lens implant power calculation formula," J. Cataract Refract. Surg. **16**(3), 333–340 (1990).
4. D. R. Sanders, J. Retzlaff, and M. C. Kraff, "Comparison of the SRK II formula and other second generation formulas," J. Cataract Refract. Surg. **14**(2), 136–141 (1988).
5. G. Heron and B. Winn, "Binocular accommodation reaction and response times for normal observers," Ophthalmic Physiol. Opt. **9**(2), 176–183 (1989).
6. H. Radhakrishnan and W. N. Charman, "Age-related changes in ocular aberrations with accommodation," J. Vis. **7**(7), 11 (2007).
7. E. J. Fernández and P. Artal, "Study on the effects of monochromatic aberrations in the accommodation response by using adaptive optics," J. Opt. Soc. Am. A **22**(9), 1732–1738 (2005).
8. L. N. Davies, M. A. Croft, E. Papas, and W. N. Charman, "Presbyopia: physiology, prevention and pathways to correction," Ophthalmic Physiol. Opt. **36**(1), 1–4 (2016).
9. A. Glasser and M. C. W. Campbell, "Presbyopia and the optical changes in the human crystalline lens with age," Vision Res. **38**(2), 209–229 (1998).
10. H. B. Dick, "Accommodative intraocular lenses: current status," Curr. Opin. Ophthalmol. **16**(1), 8–26 (2005).
11. R. Menapace, O. Findl, K. Kriechbaum, and Ch. Leydolt-Koeppl, "Accommodating intraocular lenses: a critical review of present and future concepts," Graefes Arch. Clin. Exp. Ophthalmol. **245**(4), 473–489 (2007).
12. I. G. Pallikaris, G. A. Kontadakis, and D. M. Portaliou, "Real and pseudoaccommodation in accommodative lenses," J. Ophthalmol. **2011**, 284961 (2011).
13. O. Findl and C. Leydolt, "Meta-analysis of accommodating intraocular lenses," J. Cataract Refract. Surg. **33**(3), 522–527 (2007).
14. S. Marcos, S. Ortiz, P. Pérez-Merino, J. Birkenfeld, S. Durán, and I. Jiménez-Alfaro, "Three-dimensional evaluation of accommodating intraocular lens shift and alignment in vivo," Ophthalmology **121**(1), 45–55 (2014).

#288053 https://doi.org/10.1364/BOE.8.002396
Journal © 2017 Received 8 Mar 2017; revised 31 Mar 2017; accepted 2 Apr 2017; published 5 Apr 2017

Biomedical Optics EXPRESS

15. W. N. Charman, "Developments in the correction of presbyopia II: surgical approaches," Ophthalmic Physiol. Opt. **34**(4), 397–426 (2014).
16. E. Rosen, J. L. Alió, H. B. Dick, S. Dell, and S. Slade, "Efficacy and safety of multifocal intraocular lenses following cataract and refractive lens exchange: Metaanalysis of peer-reviewed publications," J. Cataract Refract. Surg. **42**(2), 310–328 (2016).
17. P. Artal, "History of IOLs that correct spherical aberration," J. Cataract Refract. Surg. **35**(6), 962–963, author reply 963–964 (2009).
18. P. Artal, E. Berrio, A. Guirao, and P. Piers, "Contribution of the cornea and internal surfaces to the change of ocular aberrations with age," J. Opt. Soc. Am. A **19**(1), 137–143 (2002).
19. P. Artal, A. Guirao, E. Berrio, and D. R. Williams, "Compensation of corneal aberrations by the internal optics in the human eye," J. Vis. **1**(1), 1 (2001).
20. P. A. Piers, E. J. Fernandez, S. Manzanera, S. Norrby, and P. Artal, "Adaptive optics simulation of intraocular lenses with modified spherical aberration," Invest. Ophthalmol. Vis. Sci. **45**(12), 4601–4610 (2004).
21. J. Tabernero, P. Piers, A. Benito, M. Redondo, and P. Artal, "Predicting the optical performance of eyes implanted with IOLs to correct spherical aberration," Invest. Ophthalmol. Vis. Sci. **47**(10), 4651–4658 (2006).
22. P. Artal, S. Manzanera, P. Piers, and H. Weeber, "Visual effect of the combined correction of spherical and longitudinal chromatic aberrations," Opt. Express **18**(2), 1637–1648 (2010).
23. H. A. Weeber and P. A. Piers, "Theoretical performance of intraocular lenses correcting both spherical and chromatic aberration," J. Refract. Surg. **28**(1), 48–52 (2012).
24. C. Schwarz, C. Cánovas, S. Manzanera, H. Weeber, P. M. Prieto, P. Piers, and P. Artal, "Binocular visual acuity for the correction of spherical aberration in polychromatic and monochromatic light," J. Vis. **14**(2), 1 (2014).
25. S. Ravikumar, A. Bradley, and L. N. Thibos, "Chromatic aberration and polychromatic image quality with diffractive multifocal intraocular lenses," J. Cataract Refract. Surg. **40**(7), 1192–1204 (2014).
26. B. Cochener; Concerto Study Group, "Clinical outcomes of a new extended range of vision intraocular lens: International Multicenter Concerto Study," J. Cataract Refract. Surg. **42**(9), 1268–1275 (2016).
27. N. E. de Vries and R. M. Nuijts, "Multifocal intraocular lenses in cataract surgery: literature review of benefits and side effects," J. Cataract Refract. Surg. **39**(2), 268–278 (2013).
28. F. Vega, F. Alba-Bueno, M. S. Millán, C. Varón, M. A. Gil, and J. A. Buil, "Halo and through-focus performance of four diffractive multifocal intraocular lenses," Invest. Ophthalmol. Vis. Sci. **56**(6), 3967–3975 (2015).
29. K. Kamiya, K. Hayashi, K. Shimizu, K. Negishi, M. Sato, and H. Bissen-Miyajima; Survey Working Group of the Japanese Society of Cataract and Refractive Surgery, "Multifocal intraocular lens explantation: a case series of 50 eyes," Am. J. Ophthalmol. **158**(2), 215–220.e1 (2014).
30. H. L. Liou and N. A. Brennan, "Anatomically accurate, finite model eye for optical modeling," J. Opt. Soc. Am. A **14**(8), 1684–1695 (1997).
31. I. Escudero-Sanz and R. Navarro, "Off-axis aberrations of a wide-angle schematic eye model," J. Opt. Soc. Am. A **16**(8), 1881–1891 (1999).
32. D. A. Atchison and G. Smith, "Chromatic dispersions of the ocular media of human eyes," J. Opt. Soc. Am. A **22**(1), 29–37 (2005).
33. G.-Y. Yoon and D. R. Williams, "Visual performance after correcting the monochromatic and chromatic aberrations of the eye," J. Opt. Soc. Am. A **19**(2), 266–275 (2002).
34. Y. Benny, S. Manzanera, P. M. Prieto, E. N. Ribak, and P. Artal, "Wide-angle chromatic aberration corrector for the human eye," J. Opt. Soc. Am. A **24**(6), 1538–1544 (2007).
35. K. Ohnuma, H. Kayanuma, T. Lawu, K. Negishi, T. Yamaguchi, and T. Noda, "Retinal image contrast obtained by a model eye with combined correction of chromatic and spherical aberrations," Biomed. Opt. Express **2**(6), 1443–1457 (2011).

1. Introduction

Intraocular lenses (IOLs) are surgically implanted in the eye to replace the crystalline lens in cataract surgery. Adequate lens power for each eye is determined by formulas fitted with biometric parameters of the patient's eye. Some empirical parameters are also introduced enhancing the output [1–4]. The surgical replacement of the crystalline lens has achieved an acceptable success rate. For most pseudophakic patients, the final refraction for far vision is below one diopter. Both defocus and astigmatism can be largely reduced after IOL implantation for any patient, avoiding the dependency of glasses for far vision. A significant limitation of conventional monofocal IOLs is the lack of change in power once implanted in the eye. The sharp vision of intermediate and near objects would require the addition of power in the IOL. This is occurring in the young crystalline lens, commonly referred to as accommodation [5–7]. The progressive loss of accommodation with age is called presbyopia [8,9]. Typically, most cataract patients implanted with IOLs are already presbyopic subjects. In this situation, glasses or similar optical aids become still necessary for intermediate and

Biomedical Optics EXPRESS

near vision. Different optical solutions incorporated to IOLs have been proposed to correct for this lack of accommodation. Accommodative IOLs are intended to change the eye power [10,11], although their actual implementation has not been successful yet [12–14]. Other IOLs incorporated multifocality, distributing the light in the image plane across separated foci [15,16]. Those lenses partially ameliorate vision at closer distances, but at the cost of also reducing the contrast and some patients report discomfort under low illumination. An important advance in the field of IOL design was the incorporation of aspheric surfaces [17]. It allowed partially compensating the average spherical aberration of the aged eye [18–21]. Moreover, the controlled manipulation of the spherical aberration of the pseudophakic eye, beyond its pure correction, has been proven to extend the depth of focus [21].

Another option to further improve retinal image quality is the use of achromatic IOLs designed to correct for chromatic aberration of the eye [22–24]. Previous achromatic IOLs have been based in the use diffractive surfaces [25,26]. Although, diffractive IOLs are widely used specially in multifocal lenses, they usually present some drawbacks, due to parasitic foci that can reduce contrast and generate the perception of halos and other dysphotopsias [27,28]. The discomfort can be in certain cases so important, that some patients even require undergoing surgery to exchange the diffractive IOL [29].

In this context, we present a different approach for correcting chromatic aberration by using a doublet IOL composed of two materials, and then avoiding diffractive surfaces. The new lens is also designed to correct for monochromatic higher order aberrations, including spherical aberration. This correction is performed on an extended retinal patch.

2. Methods

A chromatic eye model was used to reproduce the chromatic aberration, higher-order aberrations, and provides realistic values for off-axis aberrations within a retinal eccentricity of 10 degrees. The parameters of the eye model are shown in the Table 1. This was based in previously published eye models [30,31] with the values of dispersion and refractive indexes of the ocular media from Atchison and Smith [32].

Table 1. Eye model

Element	Radius (mm)	Thickness (mm)	Refractive index	Abbe number	Semi diameter (mm)	Conic constant
Anterior cornea	7.77	0.55	1.3766	55.7029	6	–0.18
Posterior cornea	6.4	3.16	1.3375	50.6963	6	–0.6
Iris	Infinity	0	-	-	2	0
Anterior lens	10.2	4	1.4201	50.7824	4	–3.132
Posterior lens	–6	16.032	1.3361	53.5626	4	–1
Retina	–12	-	-	-	10	0

Existing IOL materials were employed to design the lens, modeled with their refractive index and chromatic dispersion. The latter was described with the Abbe number. Two materials were used: a relatively low dispersion material A, with refractive index $n_A = 1.47$ and Abbe number $V_d(A) = 55$, and a more dispersive second material B, $n_B = 1.55$ and $V_d(B) = 37$.

Ray-tracing techniques were used to optimize the optical performance of different IOLs within the previously described eye model. An optical design software was employed (Zemax OpticStudio, Zemax LLC, USA). Once the materials were selected, a merit function was developed to design the IOLs. In general, the parameters are selected across those of relevance for the intended performance of the lens. During the optimization procedure, different values are systematically given to the independent variables. Subsequently, those are employed to calculate the selected merit function components. The target is to find a set of

Biomedical Optics EXPRESS

values for the variables which minimize the merit function. In the ideal case, the procedure finishes with the finding of a global or absolute minimum, rather of a local minimum. The merit function generated incorporated constraints for the geometrical parameters of the IOL to keep them within physiologically compatible ranges. The variable parameters for the optimization were the thickness of the lens, its position within the capsule, the radius of curvature, and the asphericity of the different surfaces. Three configurations were simultaneously included in the merit function corresponding to incoming beams on axis, at 5, and at 10 degrees of eccentricity in the horizontal direction. Polychromatic light composed by 5 equally weighted wavelengths at 450, 503, 555, 610 and 650 nm was considered. The spectral sensitivity of the photoreceptors was not included in the simulation. The selected merit function components were the angular size of the aerial image formed on the retina from a distant point object, with a target value of zero, and the longitudinal chromatic aberration for the previous wavelengths. The procedure assumed a 4-mm entrance pupil diameter in the eye.

Biometric data from two nearly emmetropic subjects were employed for testing the IOL design under realistic conditions. The subjects were 65 years old when the biometry was obtained. The biometric data included were the anterior corneal topography and the axial length of the eye.

3. Results

3.1 IOL optimization

The optimization was applied to a doublet lens made of materials A and B as well as to a single lens made of material B. The latter cannot correct chromatic aberration, but was optimized to keep the best possible optical quality at the three considered eccentricities. The lens of material B is referred to as best aspheric intraocular lens (BA-IOL). Comparison between the doublet and the BA-IOL was performed. The parameters of the doublet lens are shown in the Table 2.

Table 2. Doublet lens

Element	Radius (mm)	Thickness (mm)	Refractive index	Abbe number	Semi diameter (mm)	Conic constant
Anterior surface	12.025	1.295	1.47	55	3	2.34
Intermediate surface	–2.114	0.651	1.55	37	3	–2.671
Posterior surface	–4.161	-	-	-	3	–6.518

Figure 1 shows the chromatic shift (D) as a function of the wavelength (μm) for the visible range. The blue solid line corresponds to the eye model with the doublet lens, the red solid line for the BA-IOL, and the dashed line shows the chromatic aberration of the eye with the natural crystalline lens. The curves corresponding to the IOLs were obtained by cubic spline interpolation from data sampled at the used wavelengths.

The longitudinal chromatic aberration of the eye model implanted with the doublet IOL crosses the axis at 543 and 555 nm. In the visible range, the maximum chromatic shift for the eye implanted with the doublet is 0.025 D. The maximum shift for the natural eye and the BA-IOL is 0.96 D and 1.24 D, respectively. Lateral color was also estimated in the range of eccentricities from 0 to 10 deg for the doublet IOL (555 nm was taken as the reference wavelength). The displacement of the images as a function of wavelength exhibited a linear trend. The differences of the centroid position of the aerial images on the retina were –4.09, –1.93, 0, 1.85, and 2.94 μm for the considered wavelengths, 450, 503, 555, 610 and 650 nm, respectively.

Biomedical Optics EXPRESS

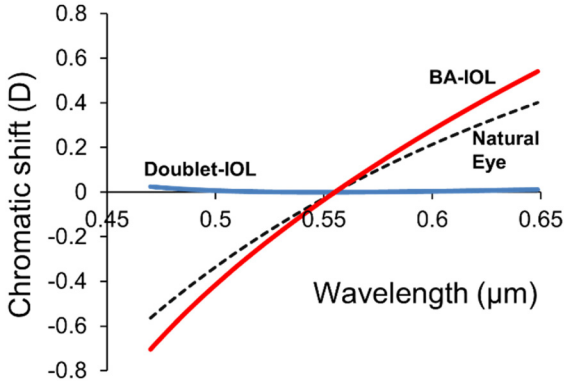

Fig. 1. Chromatic focal shift for the natural eye (dashed line), eye implanted with the doublet IOL (blue line), and eye implanted with the BA-IOL (red line).

To better understand the impact of the doublet IOL on the optical quality of the retinal images, the polychromatic point spread functions (PSF) of the pseudophakic eye model were computed. The PSFs were obtained in the range of eccentricities optimized from 0 to 10 deg, through the entrance pupil diameter of 4 mm. Part (A) of the Fig. 2 depicts the PSFs for the pseudophakic eye with the doublet (left column), and for the case of the eye model with the BA-IOL (right column). From the top to the bottom the images correspond to 0, 5 and 10 deg of eccentricity. The PSFs displayed were composed by three colors to provide a better visualization of the chromatic effect. Those colors were the standard channels green, red and blue (R, G, B) with the following associated wavelengths: 650 nm, 555 nm and 450 nm. Each frame containing a PSF corresponded to 40 μm on the retinal plane for the pseudophakic eye, around the three different eccentricities. The images on the left column exhibited a significant smaller size as compared to others on the right column. The central part of the PSFs from the pseudophakic eye with the doublet IOL showed for all eccentricities a white color spot. This is a qualitative evidence of a similar contribution to the total intensity from the three considered RGB wavelengths. In the right column, the images at the RGB colors were more separated. Because of the differences in the shape and position of the monochromatic PSFs in the case of the pseudophakic eye with the BA-IOL, white color is hardly noticeable in the images. Nevertheless, the overall size in the BA-IOL case of every polychromatic PSF was similar at the three eccentricities, showing the effect of applying the optimization.

The radial average of the polychromatic modulation transfer function (MTF) was calculated for every eccentricity up to 30 cycles/degree. The results are presented on the right panel of Fig. 2. A comparison between different MTFs can be accomplished by obtaining the ratio between the areas under the curves. The benefit of the eye implanted with the doublet-IOL, in terms of the MTF ratio, as compared with the case of BA-IOL was 1.9, 1.8, and 1.5 for 0, 5 and 10 degrees of eccentricity, respectively. The average benefit for all eccentricities was 1.76. The maximum benefit was obtained at 12.2 ± 1.7 cycles/degree. The previous value was obtained from the average for the three eccentricities.

Biomedical Optics EXPRESS

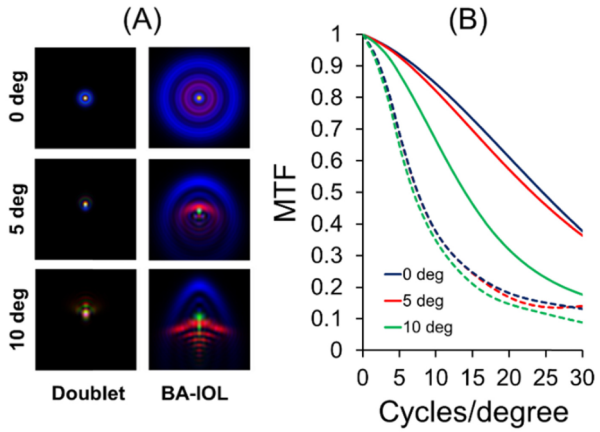

Fig. 2. (A) PSFs obtained for a pupil of 4 mm of diameter in the pseudophakic eye model implanted with the doublet IOL (left column), and the BA-IOL (right column). PSFs were calculated at the eccentricities 0, 5 and 10 deg. (B) Radial averages of the polychromatic MTFs for the entrance pupil of 4 mm corresponding to the eye model with the doublet IOL (solid lines), and with the BA-IOL (dashed lines).

The through-focus radial average of the polychromatic MTF was calculated for both the pseudophakic eye model with the doublet IOL, and with the BA-IOL. A range of 1.5 D centered at the best focal plane was chosen. The Fig. 3 shows the results. The spatial frequencies 3, 6, 12 and 18 cycles/degree were selected. The panel (A) of the Fig. 3 shows the results for the model eye implanted with the doublet IOL, while the panel (B) depicts the results for the eye with BA-IOL.

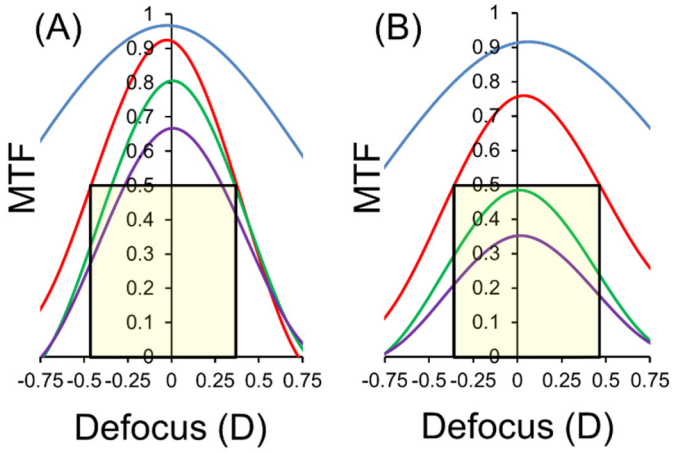

Fig. 3. Radial averages of the MTFs through focus for different spatial frequencies (3, 6, 12 and 18 c/deg; blue, red, green and purple lines respectively), in the pseudophakic eye implanted with the doublet IOL (A); and with the BA-IOL (B). Pupil size was 4 mm of diameter in all cases.

For better comparison, a rectangle was overlapped on the plots indicating the 0.5 modulation, and limited by the curve of the 6 cycles/degree. The width of the rectangle was approximately 0.82 D in both panels. In the case of the eye with the doublet IOL design, the other considered spatial frequencies were above the area of the rectangle. However, in panel (B) the spatial frequencies higher than 6 cycles/degree were under the area of the rectangle. The ratios of the areas under the polychromatic MTFs through focus were obtained in the

Biomedical Optics EXPRESS

range covered by the rectangle. There was found a better performance for the eye with the doublet IOL design, in terms of the area ratio across frequencies, of 1.04, 1.04, 1.58, and 1.83 for 3, 6, 12 and 18 cycles/degree, respectively. The higher spatial frequencies benefited more of the correction of the chromatic aberration, while practically no change was measured for lower frequencies.

3.2 Performance of the IOLs on real pseudophakic eyes

Figure 4 presents the radial averaged polychromatic MTFs obtained for each subject at 4 mm pupil diameter and three eccentricities (0, 5, and 10 degrees). The dashed lines represented the results obtained with the eyes virtually implanted with BA-IOL, being the solid lines for those from the eyes with the doublet IOL. The black curve indicated the average result from the three eccentricities of 0, 5, and 10 deg. For both subjects, the MTFs of the doublet IOL show higher values. That was also numerically characterized in terms of the ratios across the areas below the MTF curves. There were obtained 1.607 and 1.341 for subjects 1 and 2, respectively. The maximum benefit was found at 9 and 16 c/deg for each subject. For subject 2 there was not difference in the curves of the two types of IOLs until approximately the spatial frequency 5 c/deg. The MTFs corresponding to the different eccentricities run relatively similar for each type of IOL, irrespectively of the subject. An analysis of this feature was performed in terms of the standard deviation of the obtained average (black curves), as an estimation of the dispersion of the curves. For subject 1 it was obtained 0.044 and 0.014 for the cases of doublet IOL and BA-IOLs, respectively. That indicated that the BA-IOL produced more similar results at different eccentricities, though still well below the curves showing the doublet IOL. For the other subject 2 the results for the standard deviation showed a different trend, with 0.025 and 0.027 for the doublet IOL and BA-IOL, respectively.

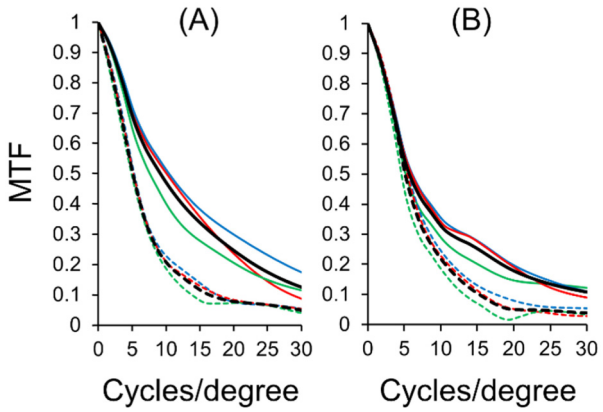

Fig. 4. Radial averages of the polychromatic MTFs for retinal eccentricities 0, 5 and 10 c/deg (in blue, red and green color, respectively) for the eye implanted with the doublet IOL (solid lines) and the BA-IOL (dashed lines) in subject 1 (panel A) and 2 (panel B).

A similar analysis on the MTFs through focus was conducted with the pseudophakic eyes models from the 2 subjects. The defocus range was set to ± 0.75 D around the retinal plane. The Fig. 5 shows graphically the results for the subjects 1 and 2, corresponding to panel (A) and (B), respectively. Solid lines indicated the results for the eyes implanted with the doublet IOL, while the dashed curves were designated for those eye models with BA-IOL. The benefit was again obtained through the ratio across corresponding MTFs areas. Subject 1 scored the following values: 1.10, 1.37, 1.85, and 2.00 for 3, 6, 12 and 18 c/deg. The average benefit of the doublet IOL as compared with the other was 1.56. The results of the ratio between MTF areas for the subject 2 were 1.19, 0.91, 1.39 and 1.62 for 3, 6, 12 and 18 c/deg. The average benefit was 1.28, in favor of the doublet IOL. It should be noticed that for this

Biomedical Optics EXPRESS

last subject, the frequency of 6 c/deg produced a value for the ratio between MTFs below 1, showing a different trend than the rest of data.

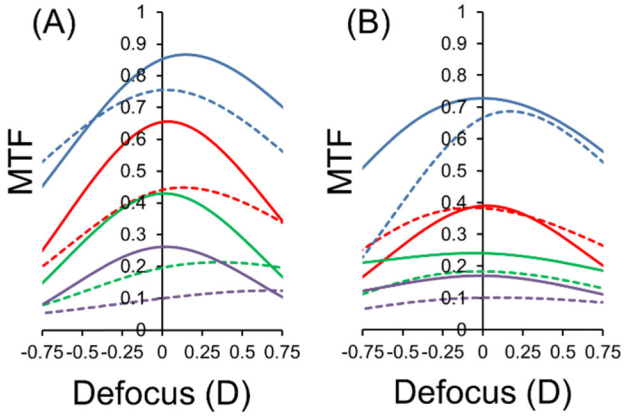

Fig. 5. Radial averages of the geometrical MTFs through focus for different spatial frequencies (3, 6, 12 and 18 c/deg in blue, red, green and purple color, respectively), in the pseudophakic eye implanted with the doublet IOL (solid curves), and with the BA-IOL (dashed curves). Each panel corresponds to a different subject. Pupil size was 4 mm of diameter in all cases.

4. Discussion

The model for optimizing the IOLs was a combination of eye models [30,31] and the dispersion and refractive indexes of the ocular media [32]. The Liou-Brennan eye model presents a crystalline lens with gradient index distribution, emulating the real lens. However, the chromatic dispersion of such gradient index crystalline lens model has not been characterized. Therefore, the longitudinal chromatic aberration of the entire eye model is not rigorously defined. For such reason, the geometrical parameters for the crystalline lens provided by Escudero-Sanz-Navarro [31] were implemented in our model. The model of Escudero-Sanz-Navarro was intended and proven to reproduce off-axis aberrations accurately. It is essentially a variation of the Liou-Brennan eye model with a simpler crystalline lens, described with a single effective refractive index. We studied different sets of dispersions and refractive indexes for the ocular media proposed in the available bibliography. The data provided by Atchison and Smith, merged with the Liou-Brennan eye model and the crystalline lens by Navarro, produced the best agreement between theory and actual measurements of longitudinal chromatic aberration in the human eye. We suggest the presented chromatic eye model as a useful alternative.

The IOL materials were described in terms of their refractive indexes and Abbe numbers. The chromatic dispersion of a material is in general a function of several parameters. A useful representation is given for instance by the Sellmeier equation, that provides the complete information about dispersion. The Abbe number provides a useful single value from the equation, allowing the comparison between dispersions. We have simplified the material description in our model by using the Abbe number. A more rigorous approach might require the employment of the full Sellmeier, or equivalent, equation. Nevertheless, if standard materials are considered the results obtained in this work by only considering Abbe numbers will not significantly differ from reality.

In the calculations of the polychromatic PSFs all wavelengths in the visible range were considered. However, only 3 colors were displayed in the PSFs on the Fig. 2. The authors tried different combinations for better showing the impact of the multiple wavelengths on the polychromatic PSFs. Finally, we adopt the RGB display as the best qualitative approach to present the results. The Fig. 2 was complemented with polychromatic MTFs to provide quantitative results to the readers. Those MTFs again were calculated with the entire visible

Biomedical Optics EXPRESS

range. In these simulations, the spectral sensitivity spectral sensitivity of the photoreceptors was not included. This Gaussian-like function weights the spectrum with the retinal response to different colors. The tails of the retinal spectral sensitivity function, towards the red and blue part of the spectrum, are largely reduced as compared with the central peak around 555 nm. We have focused on studying the retinal images form an optical perspective. The visual impact of the chromatic aberration is possibly ameliorated by this fact. However, the correction of chromatic aberration clearly allows the energy from all visible wavelengths to be merged on the same retinal plane. That should have an impact in the contrast of the images, improving vision. Some previous works have already measured this improvement [22,33–35].

The incorporation of real data from corneal topography and axial lengths to the simulations reproduced in some extent the benefits of using the doublet IOL found in the general chromatic eye model. In the real pseudophakic eyes models, the higher order aberrations beyond spherical aberration introduced some variability in the results. For instance, the benefit of the doublet IOL as compared with the BA-IOL, calculated through the ratio between MTFs, was on average from the two subjects 1.474 (1.607 and 1.341 for subjects 1 and 2, respectively), while for the chromatic eye model was 1.761. We expected this inter-subject variability to occur, still maintaining a reasonable benefit when using the doublet IOL. Data from astigmatic subjects were excluded for the pseudophakic eye models. The reason was to avoid the simulation of a toric IOL to better isolate the effect of chromatic aberration and off-axis aberrations. Nevertheless, there are no fundamental issues to develop such toric, doublet IOL.

5. Conclusions

A new design of intraocular lens for correcting chromatic, spherical, and off-axis aberrations in the pseudophakic eye has been presented. It is based in the concept of a doublet IOL and shows the potential for a near perfect aberration correction, avoiding the use of diffractive surfaces. The investigation of the impact of correcting the chromatic and monochromatic aberrations on the depth of focus was studied in this paper. The doublet IOL may provide an important optical benefit, even in the presence of typical higher order ocular aberrations. The concept developed on the doublet IOL could be also adapted to multifocal and accommodating IOLs to achieve a superior optical quality of the retinal images, in addition to their performances.

Funding

European Research Council (Advanced Grant ERC-2013-AdG-339228 (SEECAT)); Secretaría de Estado e Investigación, Desarrollo e Innovación (SEIDI) (FIS2016-76163-R); Fundación Séneca-Agencia de Ciencia y Tecnología de la Región de Murcia (grants 18964/JLI/13 and 19897/GERM/15); and the European Regional Development Fund (EU-FEDER).

Acknowledgments

Some parts and concepts of this work have been submitted as patent applications by the authors.